International Journal of Biological Macromolecules 271 (2024) 132563

Contents lists available at ScienceDirect

International Journal of Biological Macromolecules

journal homepage: www.elsevier.com/locate/ijbiomac

PLGA nanoparticle-encapsulated lysostaphin for the treatment of *Staphylococcus aureus* infections

Guillermo Landa [a,b,c,*], Laura Aguerri [a,b], Silvia Irusta [a,b,c], Gracia Mendoza [c,d,**], Manuel Arruebo [a,b,c]

[a] Instituto de Nanociencia y Materiales de Aragón (INMA), CSIC-Universidad de Zaragoza, 50009 Zaragoza, Spain
[b] Department of Chemical and Environmental Engineering, University of Zaragoza, Campus Río Ebro-Edificio I+D, C/Poeta Mariano Esquillor S/N, 50018 Zaragoza, Spain
[c] Aragon Health Research Institute (IIS Aragon), 50009 Zaragoza, Spain
[d] Department of Pharmacology and Physiology, Forensic and Legal Medicine, University of Zaragoza, 50009 Zaragoza, Spain

ARTICLE INFO

Keywords:
Staphylococcus aureus
Biofilm
Intracellular infection
Lysostaphin
PLGA nanoparticles

ABSTRACT

Staphylococcus aureus possesses the ability to become pathogenic, leading to severe and life-threatening infections. Its methicillin-resistant variant MRSA has garnered high-priority status due to its increased morbidity and associated mortality. This emphasizes the urgency for novel anti-staphylococcal agents. The bacteriocin lysostaphin stands out for its remarkable bactericidal activity against *S. aureus*, including MRSA, outperforming conventional antibiotics. However, the clinical application of lysostaphin faces challenges, including enzymatic activity loss under physiological conditions and potential immunogenicity. This study introduces a novel approach by encapsulating lysostaphin within polylactic-*co*-glycolic acid (PLGA) nanoparticles, a biodegradable copolymer known for its biocompatibility and sustained drug release ability. The study assesses the antimicrobial activity of lysostaphin-loaded PLGA nanoparticles against different *S. aureus* strains, and we also used GFP-expressing *S. aureus* for facilitating its traceability in planktonic, biofilm, and intracellular infection models. The results showed the significant reduction in bacteria viability both in planktonic and biofilm states. The *in vitro* intracellular infection model demonstrated the significantly enhanced efficiency of the developed nanoparticles compared to the treatment with the free bacteriocin. This research presents lysostaphin encapsulation within PLGA nanoparticles and offers promising avenues for enhancing lysostaphin's therapeutic efficacy against *S. aureus* infections.

1. Introduction

Staphylococcus aureus, a Gram-positive bacterium, typically exists as a commensal organism on the human skin and mucous membranes. It is calculated that ~30 % of healthy people colonized by *S. aureus* do not exhibit any pathological symptoms [1]. However, it possesses the capacity to become pathogenic under certain circumstances, giving rise to millions of severe and potentially life-threatening infections around the world [2]. According to a study conducted in 2019, *S. aureus* emerged as a primary contributor to bacterial-related deaths in 135 countries and was particularly notable for causing the highest number of infection-associated deaths among individuals aged 15 years and older worldwide [3]. *S. aureus* demonstrates a wide range of disease manifestations, including foodborne toxin infections, skin and soft tissue infections, urinary tract infections, pneumonia, endocarditis, and meningitis, among others [4–6].

Broad-spectrum antibiotics have played a crucial role in combating *S. aureus* infections over the years [7]. Nevertheless, the emergence of methicillin-resistant *S. aureus* (MRSA) has been alarming since it was first reported in the 1960s [8]. MRSA, among other antimicrobial-resistant microorganisms, is becoming increasingly ubiquitous in clinical settings becoming one of the most prevalent pathogens in healthcare-associated infections [9]. Currently, MRSA is classified as a high-priority pathogen in the World Health Organization's (WHO) list of antimicrobial resistant bacteria [10]. Consequently, there is an urgent need for novel anti-staphylococcal agents to overcome this concern.

* Correspondence to: G. Landa, Instituto de Nanociencia y Materiales de Aragón (INMA), CSIC-Universidad de Zaragoza, 50009 Zaragoza, Spain.
** Correspondence to: G. Mendoza, Aragon Health Research Institute (IIS Aragon), 50009 Zaragoza, Spain
E-mail addresses: glanda@unizar.es (G. Landa), gmendoza@iisaragon.es (G. Mendoza).

https://doi.org/10.1016/j.ijbiomac.2024.132563
Received 7 April 2024; Received in revised form 15 May 2024; Accepted 20 May 2024
Available online 21 May 2024

There is also a growing focus on selective treatments that exclusively target pathogenic bacterial species, minimizing collateral damage to commensal bacteria, promoting a healthy microbial balance in the host and boosting the immune system.

Bacteriocins, lytic enzymes of bacterial origin, serve as natural antimicrobial agents that play a crucial role in microbial competition and shaping bacterial populations [11]. Produced by bacteria as a defense mechanism against competing microorganisms, they exhibit bactericidal activity comparable to antibiotics, but with a very narrow spectrum of activity. This, coupled with their reported rarity in resistance development, make them a favorable option for antimicrobial therapy [12]. Lysostaphin (LYS), a well-studied bacteriocin, is a naturally occurring endopeptidase derived from *Staphylococcus simulans*. It possesses exceptional enzymatic activity by cleaving polyglycine bridges that serve as cross-linkers in the cell wall structure of staphylococci [13,14]. *In vitro* investigations have demonstrated its potent bactericidal efficacy against *S. aureus* strains, even those exhibiting resistance to conventional antibiotics like MRSA [15,16]. LYS displays superior efficacy compared to native human response against infection and broad-spectrum antibiotics like penicillin and vancomycin [17–19]. Furthermore, it exhibits a remarkable capability to effectively lyse both actively growing cells and cells in stationary growth phase, and shows enhanced efficacy against bacterial biofilms [15,20,21]. The effectiveness of LYS and its therapeutic potential have been examined across diverse contexts, like animal models featuring systemic infections [22], wound infections [23], bone infections [24], endocarditis [25], mastitis [21], keratitis [26], and biofilm and implant-associated infections [27]. Additionally, clinical trials have been conducted to investigate the effectiveness of LYS in humans afflicted with persistent nasal colonization [28,29]. Overall, these studies reveal the potential of LYS as a therapeutic agent against staphylococcal infections in diverse clinical scenarios.

Nevertheless, the clinical applicability of LYS encounters two primary challenges. Firstly, the loss of enzymatic activity under physiological conditions [30]. Secondly, the potential immunogenicity of LYS raises concerns regarding the development of immune responses and associated adverse reactions [31]. To overcome these challenges, a range of strategies have been explored. These strategies include PEGylation [32–34], glycosylation [35], inclusion in hydrogels [34], polymers [36], fusion with other proteins (bovine serum albumin (BSA), cell penetrating peptides (CPPs)) [37–41] or its encapsulation in different nanocarriers such as liposomes [42].

Encapsulation of enzymes within polymeric particles offers a promising approach to preserve their stability and to ensure the sustained enzymatic activity required for effective therapeutic applications [43,44]. By providing a protective environment, this platform may preserve and maintain the enzymatic functionality over extended periods of time [45,46]. In this study, we present a novel approach for enhancing the efficacy of LYS by encapsulating it within Polylactic-*co*-glycolic acid (PLGA) nanoparticles. This copolymer is present in several FDA and EMA-approved drug delivery systems and medical devices due to its remarkable biocompatibility and biodegradability, being extensively employed as a controlled drug-release polymer. Its utilization, particularly when formulated into micro or nano-sized particles, finds broad applications *in vitro* and *in vivo* for the delivery of antibiotics, proteins, nucleic acids and so on [47]. In this work, we have focused on the evaluation of the antimicrobial activity of LYS-loaded PLGA nanoparticles against *S. aureus* in both planktonic and sessile states, as well as in an intracellular infection model in J774 murine macrophages. Intracellular bacterial persisters are responsible for episodes of infection relapse and their elimination is challenging. This research aims to shed light on the potential of this formulation in improving the therapeutic efficacy of LYS, thereby addressing the challenges associated with intracellular *S. aureus* infections.

2. Materials and methods

2.1. Materials

Poly(lactic-*co*-glycolic acid) (PLGA) 50:50 Resomer RG 502H was purchased from Evonik Industries AG (Essen, Germany). Recombinant lysostaphin from *Staphylococcus simulans* (LYS; ≥90 %; 3,000 UN/mg), 2,2,2-trifluoroethanol (TFE), dichloromethane (DCM), Mowiol® 4–88 (PVA), BSA, acetic acid, Calcofluor White and Crystal Violet ACS reagent were supplied by Sigma Aldrich (Darmstadt, Germany). *S. aureus* ATCC 25923 strain was obtained from Ielab (Alicante, Spain). *S. aureus* GFP was kindly donated by Dr. Iñigo Lasa and obtained using a pCN47 plasmid carrying a Phyper constitutive promoter as reporter of the GFP and grown with 10 μg/mL erythromycin. Moreover, two clinical strains (methicillin-susceptible *S. aureus* (MSSA) Newman strain and methicillin-resistant *S. aureus* (MRSA) USA300 strain) were kindly donated by Dr. Cristina Prat (Institut d'Investigació en Ciències de la Salut Germans Trias i Pujol, Badalona, Spain). Paraformaldehyde (PFA) 4 % in PBS and Phalloidin-546 were obtained from Fisher Scientific (Waltham, MA, USA). The Blue® Cell Viability Assay kit was purchased from Abnova (Taipei, Taiwan) while saponin from Quillaja Bark pure and SDS for molecular biology were obtained from AppliChem (Germany). Fetal bovine serum (FBS) was obtained from Gibco (Waltham, MA, USA) while high-glucose Dulbecco's modified Eagle's medium (DMEM w/stable glutamine), antibiotic-antimycotic solution (penicillin-streptomycin-amphotericin B; PSA) and DPBS 1× buffer were acquired from Biowest (Nuaillé, France). Tryptone soy broth (TSB) was obtained from Laboratorios Conda-Pronadisa SA (Madrid, Spain) and tryptone soy agar plates (TSA) were purchased from Avantor VWR (Radnor, PA, USA).

2.2. Synthesis of PLGA@LYS nanoparticles

To prepare the PLGA@LYS nanoparticles (NPs), a LYS aqueous solution (2 mg/mL, 0.5 mL) was combined with TFE:DCM (1:4, 4.5 mL) in which PLGA (100 mg) had been previously dissolved. The resulting solution was added dropwise into a 5 % (*w/v*) PVA aqueous solution. To form an emulsion, the mixture was sonicated using a probe with a diameter of 0.13 in. and an amplitude of 40 % (Digital Sonifier 450, Branson, MO, USA). The emulsion was allowed to stir at room temperature for 4 h to allow DCM and TFE evaporation and the subsequent precipitation of the NPs. To remove the excess of PVA and unincorporated LYS, the resulting NPs were centrifuged at 13,000 rpm for 15 min and washed three times with ultrapure water.

2.3. Characterization of PLGA@LYS NPs

Particle size and size distribution of PLGA@LYS NPs were measured by dynamic light scattering (DLS) using a Brookhaven 90Plus particle size analyzer. For zeta potential measurements, the same equipment with ZetaPALS software was employed. The assays were conducted in a 1 mM KCl aqueous solution at a pH of 6, maintaining a stable temperature of 25 °C. The zeta potential values were ascertained by examining the electrophoretic mobility of NPs and subsequently applying the Smoluchowski equation. The morphology of the NPs was visualized using a FEI inspect F50 scanning electron microscope (SEM; FEI company, Hillsboro, OR, USA) after sputter coating the particles with Pd. To determine the concentration (μg/mL) of PLGA@LYS NPs in an aqueous suspension for further experiments, a defined volume of the suspension was weighed and then evaporated in a 60 °C oven before measuring the weight of the dried residue with a microbalance and its concentration calculated by mass balance. Encapsulation efficiency (EE) and drug loading (DL) of LYS into PLGA NPs were determined by using a modified BCA Protein Assay Kit (Thermo Fisher Scientific). Briefly, the NPs were dissolved in an aqueous solution containing 0.1 M NaOH 0.5 % (*w/v*) and stirred vigorously during 24 h at 37 °C to hydrolyze completely the

PLGA and release the LYS. Prior to the assay, the samples were sonicated for 15 min and then centrifuged 5 min at 13,000 rpm to collect the supernatants. LYS was quantified using a Varioskan LUX microplate reader (Thermo Fisher Scientific) at a wavelength of 595 nm. The EE and DL in the different formulations were calculated using Eqs. (1) and (2):

$$EE\ (\%) = \frac{mass\ of\ encapsulated\ LYS\ (mg)}{mass\ of\ added\ LYS\ (mg)} x100 \quad (1)$$

$$DL\ (\%) = \frac{mass\ of\ encapsulated\ LYS\ (mg)}{total\ mass\ of\ PLGA@LYS\ NPs\ (mg)} x100 \quad (2)$$

To determine the drug release profile of LYS from the PLGA@LYS NPs, the samples were dispersed in a PBS buffer solution and incubated at 37 °C with constant agitation. At predefined time points, aliquots of the suspension were collected and centrifuged (5 min, 13,000 rpm) to obtain the supernatant. The amount of released LYS was quantified using the BCA assay. The percentage of released LYS was calculated with respect to the total amount of protein encapsulated in the NPs. The experiment was performed in triplicate.

2.4. Antimicrobial activity of free LYS and PLGA@LYS NPs

Different strains of *S. aureus* (ATCC 25923, GFP-expressing *S. aureus*, Newman (MSSA) and USA300 (MRSA)) were inoculated in 5 mL of TSB and incubated overnight at 37 °C with shaking. The culture was then diluted in fresh TSB to achieve a constant OD_{600} ($\approx 10^7$ colony forming units (CFU)/mL)) and transferred to a 96-well plate. Bacterial suspensions were then treated with increasing concentrations of free LYS (0.25–3 μg/mL) or PLGA@LYS NPs (10–100 μg/mL, to reach equivalent concentrations of the free antimicrobial peptide) in TSB and incubated at 37 °C for 24 h with shaking. The antibacterial activity was evaluated by the serial dilution method followed by plating the treated samples on TSA plates. The experiments were carried out three times in triplicate comparing the results obtained against those yielded from control samples (not treated samples and non-loaded PLGA NPs).

2.5. Biofilm inhibition and disruption assays

S. aureus expressing GFP was inoculated in 5 mL of TSB and incubated at 37 °C with vigorous shaking overnight. The resulting culture was diluted in fresh TSB to attain a constant OD_{600} ($\approx 10^7$ CFU/mL) and then transferred to 96-well plates. For the biofilm inhibition studies, cultures were treated at this point with increasing concentrations of free LYS (0.1–64 μg/mL) or PLGA@LYS NPs (5–2000 μg/mL, to reach equivalent concentrations of the free antimicrobial peptide) in TSB and incubated at 37 °C for 24 h without shaking. For the biofilm disruption studies, cultures were not treated and incubated at 37 °C for 24 h with shaking to promote biofilm formation. Then, planktonic cells were removed by washing twice with PBS and the already formed mature biofilms were treated at the same conditions as the ones used in the inhibition studies. In both methodologies, after incubation, samples were washed twice with PBS prior quantifying the biofilm biomass by the Crystal Violet assay, to count bacterial colonies, and to study the biofilm morphology by confocal microscopy.

As mentioned, the evaluation of the biofilm biomass obtained was carried out by the Crystal Violet assay. First, cultures were fixed with 200 μL of 4 % PFA in PBS for 15 min and then stained with 200 μL of 0.1 % Crystal Violet in Milli Q water for another 15 min. After staining, the Crystal Violet in excess was removed by washing the wells with water up to 5 times. The fixed stained samples were solubilized with 200 μL of 33 % acetic acid for 15 min. Lastly, the absorbance was measured at 570 nm using a Varioskan LUX microplate reader (Thermo Fisher Scientific). Five replicas of each experimental group were tested.

To count the bacterial colonies obtained, the biofilms were disrupted by sonication in a water bath for 5 min and collected. Finally, the dispersed biofilms were serially diluted in sterile PBS before plating them in TSA for CFU counting. The experiments were carried out three times in triplicate.

To observe the morphology of the biofilms, *S. aureus* GFP cultures were established using the same procedure described above, with the exception that bacteria were seeded onto microscope 8-cell culture chamber slides (Thermo Fisher Scientific). Then, the biofilms were stained with Calcofluor White at a concentration of 40 μg/mL for 20 min at room temperature. The stain in excess was removed by washing it three times with sterile PBS. Samples were then covered with coverslips and with a drop of mounting medium (Fluoromount-G™, Thermo Fisher Scientific). The biofilms were observed using a confocal laser scanning microscope (Zeiss LSM 880; Zeiss, Germany) equipped with a 63× oil immersion objective. *Z*-stack images were acquired with a step size of 0.5 μm, and the images were analyzed using the ZEN 3.3 software (Zeiss, Germany).

In all these assays, control samples (not treated samples and non-loaded PLGA NPs) were also evaluated.

2.6. Cell cytotoxicity assays

The cytotoxic effects of LYS and PLGA@LYS NPs were evaluated using J774 murine macrophages. The macrophages were grown in DMEM High-Glucose supplemented with 10 % FBS and 1 % PSA, and were incubated in a humidified atmosphere at 37 °C and 5 % CO_2. The medium was replaced every 2–3 days and cells were passaged when they reached confluence. For the cytotoxicity assays, the cells were seeded in 96-well plates at a density of 18,000 cells/cm^2 and incubated overnight. Then, the culture medium was replaced with fresh DMEM containing varying concentrations of LYS (0.1–16 μg/mL) and PLGA@LYS NPs (60–1000 μg/mL) and incubated for 24 h. After the incubation, cell viability was assessed using the Blue Cell Viability Assay (Abnova, Taipei, Taiwan). Briefly, the medium was replaced with 100 μL of fresh supplemented DMEM containing 10 % of the reagent and incubated for 2 h at 37 °C. The fluorescence was measured at excitation/emission wavelengths of 570/590 nm using a Varioskan LUX microplate reader (Thermo Fisher Scientific). Control samples (non-treated samples and samples treated with non-loaded PLGA NPs) were also analyzed (assigned with 100 % viability). The experiments were performed in triplicate.

2.7. In vitro model of cell infection and treatment

The *in vitro* infection model was developed as we previously reported [48]. In brief, J774 macrophages were seeded in 6-well plates at a density of 18,000 cells/cm^2. Before the infection assay, cells were washed twice with PBS and DMEM was renewed without PSA to avoid any interference with the infection.

To prepare *S. aureus* GFP, 5 mL of TSB was inoculated and incubated overnight at 37 °C with shaking. The bacteria were then cultured by centrifugation at 4000 rpm for 5 min, washed with PBS, and resuspended in the same buffer to achieve a constant OD_{600} ($\sim 10^7$ CFU/mL). To establish the co-culture of macrophages and *S. aureus* GFP, the bacterial cells were added to the macrophage culture at a multiplicity of infection (MOI) of 10:1. The co-culture was then centrifuged at 200 *g* for 5 min and incubated for 1 h at 37 °C. Subsequently, the medium was discarded, and the cells were washed with PBS to remove non-phagocytized bacteria. To eliminate any remaining extracellular bacteria, the cells were then treated with 100 ppm gentamicin in DMEM for an additional hour.

Two different approaches were used for the treatment of the intracellular infection. In the first approach, macrophages were pre-treated with various concentrations of either LYS (1 and 5 μg/mL) or PLGA@LYS NPs (50–500 μg/mL) in supplemented DMEM for 4 h prior to the infection. In the second approach, already infected macrophages were treated with the same concentrations of LYS and PLGA@LYS NPs for 1 h, replacing gentamicin. In both cases, non-infected and non-treated cells

were used as controls. The schematic diagram of the two experimental processes is shown in Fig. 1. The rationale behind was to know if LYS in its free and encapsulated forms was able to prevent eukaryotic cells for being infected (pre-treatment approach) and to know if LYS in its free and encapsulated forms was able to eliminate intracellular infective persisters (post-treatment approach).

To perform a quantitative analysis of the infection status in the co-culture, the cells underwent flow cytometry (FACS) analysis. To do this, the co-cultures were fixed with 4 % PFA for 30 min at room temperature. Afterwards, cells were washed and collected to be analyzed by FACS (Gallios flow cytometer, Beckman Coulter, USA). The cells within the co-culture were sorted based on their size and the level of GFP signal. The GFP signal was observed using an excitation wavelength of 488 nm and an emission wavelength of 525 nm. Resulting data were analyzed using the Flowing 2 software.

Additionally, confocal microscopy was used to observe the effects of LYS and PLGA@LYS NPs treatments against the intracellular *S. aureus* GFP infection in macrophages. For these experiments, the methodology followed was the same as described above though in order to facilitate microscopy analysis, a glass coverslip (Ø13 mm) was initially placed on the bottom of the multi-well plates before macrophages seeding. After cell fixation, the coverslips with the cells were incubated in the dark with Phalloidin 546 (1:200 in PBS-BSA-saponin solution) for 1 h at room temperature. Then, cells were rinsed with 1 % PBS-BSA and distilled water. Afterwards, cells were washed with PBS 1× BSA 1 %, and subsequently with a solution of saponin 0.1 % in PBS 1× BSA 1 %. The samples were then mounted on glass slides using DAPI-Fluoromount G™ (Thermo Fisher Scientific) and analyzed using confocal microscopy (Zeiss LSM 880; Zeiss, Germany) with a 63× oil immersion objective. In the case of GFP, Phalloidin 546, and DAPI, the maximum excitation and emission wavelengths were 489/508 nm, 556/570 nm, and 358/461 nm, respectively. The laser wavelengths for excitation were dynamically adjusted in real-time to prevent interference or overlaps and ensure the detection of each fluorescent label separately. *Z*-stack images were acquired with a step size of 0.5 μm, and z-stack orthogonal projections were utilized to visualize the presence of bacteria inside the macrophages. The images were analyzed using the ZEN 3.3 software (Zeiss, Germany).

In these experiments, control samples (not treated samples and non-loaded PLGA NPs) were also evaluated.

2.8. Statistical analyses

In every bar graph, values are displayed as the mean ± SD. The statistical analysis of experimental data was performed using Prism 8 software (GraphPad Software Inc., San Diego, CA, US). Three replicas were carried out for each experiment, and all experimental conditions were tested in triplicate unless otherwise specified. The statistical analysis in the antimicrobial activity experiments was performed using the Kruskal-Wallis test. For the intracellular infection assay, a one-way analysis of variance (ANOVA) was employed for conducting multiple comparisons along with a Dunnett's post-test. Statistically significant differences were identified when $p \leq 0.05$.

3. Results and discussion

3.1. Physico-chemical characterization of PLGA@LYS NPs

Fig. 2a displays the SEM micrographs obtained for the PLGA@LYS NPs. All the images obtained showed a relatively homogeneous diameter in the particles and a spherical shape. PLGA@LYS NPs exhibited mean diameters of 153.76 ± 45.8 nm. Fig. 2b shows the unequivocal absorbance signal in the UV region (max 280 nm attributed to its proteinaceous nature) of the LYS when loaded within the PLGA@LYS NPs. The synthesis method was adapted from Lin et al. [46], who synthesized PLGA microparticles encapsulating LYS using the same polymer. The

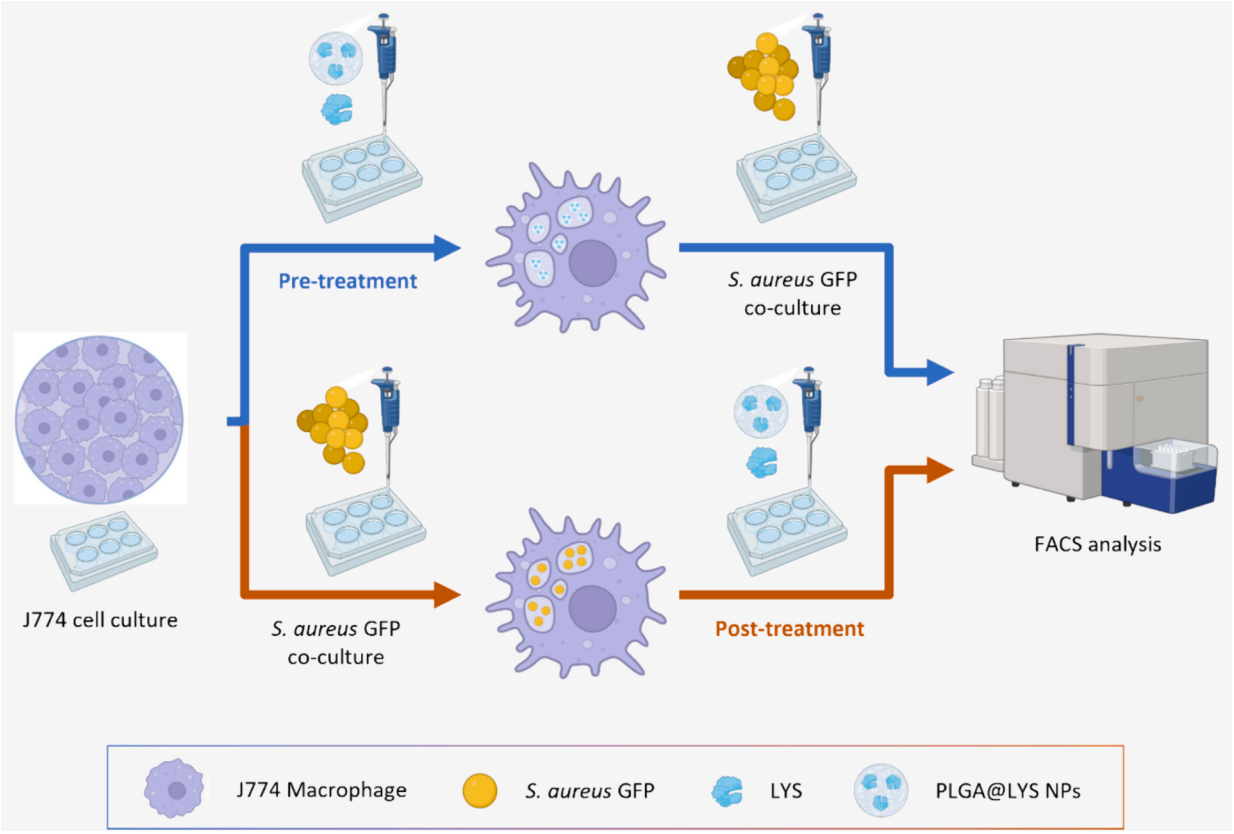

Fig. 1. Experimental methodologies following pre-treatment and post-treatment strategies.

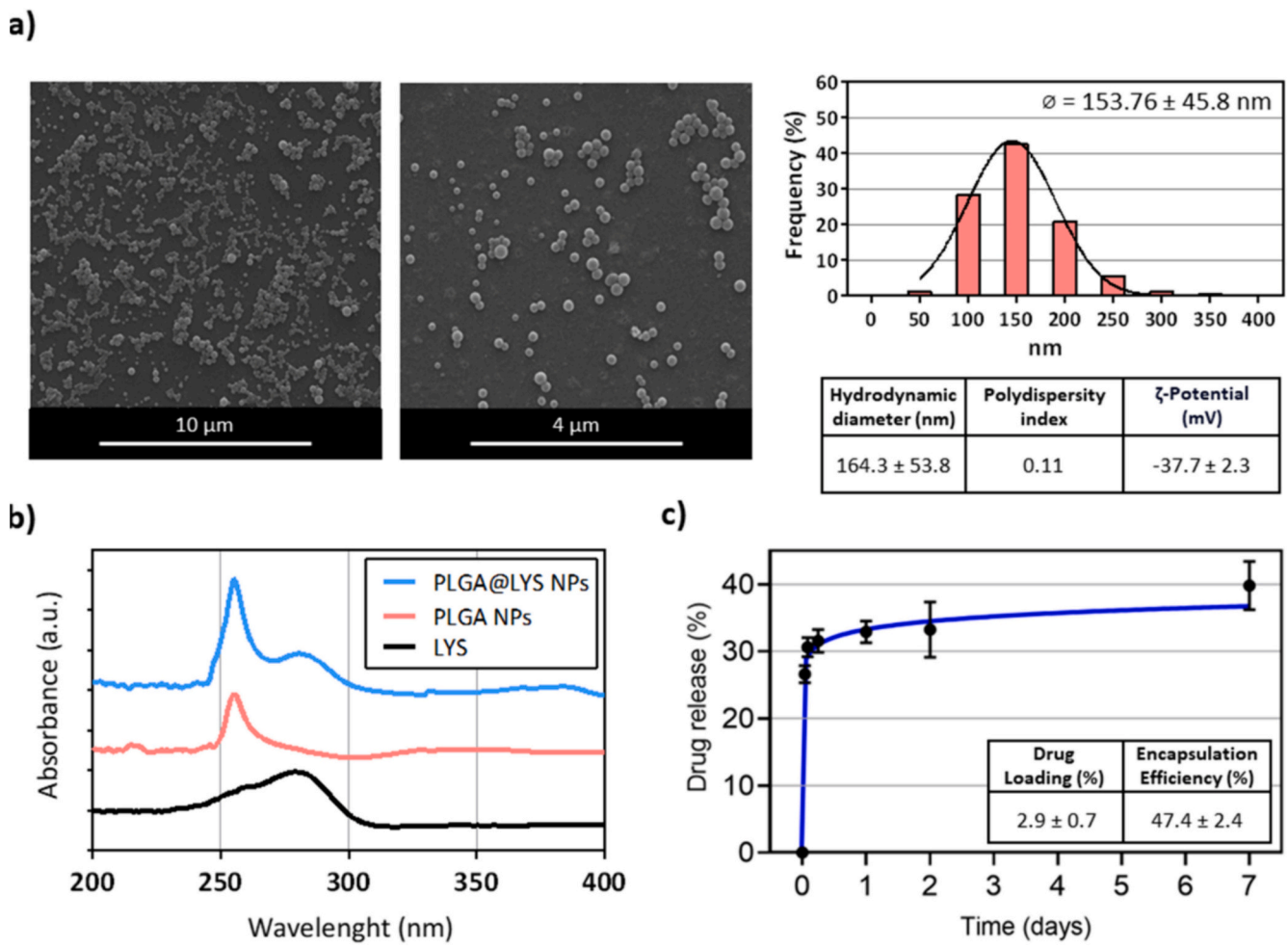

Fig. 2. Synthesis and characterization of PLGA@LYS NPs: a) SEM images of PLGA@LYS NPs and the frequency distribution of their particle diameters. The table displays the results of DLS analysis and z-potential measurements at a pH of 6; b) UV-VIS identification of LYS in PLGA@LYS NPs; c) Drug release profile of LYS from PLGA@LYS NPs and its corresponding numerical fitting using the Peppas-Sahlin model. The inset table shows the percentages of drug loading and encapsulation efficiency data.

synthesis method optimization was initially performed in the absence of LYS, using BSA (a cost-effective model protein) instead of LYS. The differences in morphology between the PLGA@LYS NPs and the empty/BSA-loaded particles were not significant (results not shown). The encapsulation efficiency and drug loading were 47.38 ± 2.4 wt% and 2.88 ± 0.7 wt%, respectively. The release kinetics of LYS from the PLGA@LYS NPs were evaluated in saline buffer. The release profile (Fig. 2c) demonstrated a two-phase pattern: an initial burst release during the first 24 h, followed by a prolonged and sustained release over a period of 7 days. At this point, 37.5 wt% of the LYS content was released. Data was reasonably well fitted to the Peppas-Sahlin model indicating that LYS release was attributed to both Fickian diffusion and case II relaxations. The rapid protein release during the initial burst is advantageous as it makes LYS rapidly bioavailable to eradicate bacteria. Meanwhile, the sustained release maintains persistent concentration levels that last for days, preventing further bacterial growth and the possibility of re-infection. This profile would be attributed to an initial release of the LYS present in the outmost part of the PLGA nanoparticles and a subsequent release of the LYS present in the solid matrix structure after hydrolysis and matrix erosion. Lin et al. reported the formulation of PLGA microparticles encapsulating LYS for pulmonary delivery [46]. Contrary to our work, those authors showed a burst release extended between 24 and 72 h, eventually reaching almost 100 % release rate after 7 days. However, our PLGA system still maintained 65 % LYS non released after 7 days, indicating a more prolonged release to inhibit potential infections mediated by persisters. According to those authors and the previous literature [49], this delayed burst release is attributed to an empty microspherical structure present in their capsules, which is something not existent in the solid matrix nanoparticles synthesized in the current study.

3.2. Antimicrobial activity

Free LYS showed a concentration-dependent antimicrobial activity against all tested *S. aureus* planktonic strains (Fig. 3a). LYS minimum bactericidal concentration (MBC) varied among the different strains, MRSA being the most susceptible (1 µg/mL), which is a positive outcome. However, these differences in susceptibility between strains are not considered significant according to previous reports [50]. The LYS MIC and MBC against *S. aureus* GFP were determined to be 0.5 and 3 µg/mL, respectively. Given that MIC values for *S. aureus* GFP were in the same order as those observed for *S. aureus* wild type (WT) and for MRSA, the former strain was used for the subsequent assays in order to take advantage of its easy visualization by confocal microscopy. The PLGA@LYS NPs also exhibited significant antimicrobial activity against planktonic *S. aureus* GFP strain, showing MIC and MBC values of 60 and 80 µg/mL. Considering the DL data (Fig. 2c), these values would correspond to approximately 1.73 and 2.3 µg/mL of encapsulated LYS. These values, while not identical to those observed for free LYS, indicate that LYS retained its bactericidal activity after the encapsulation

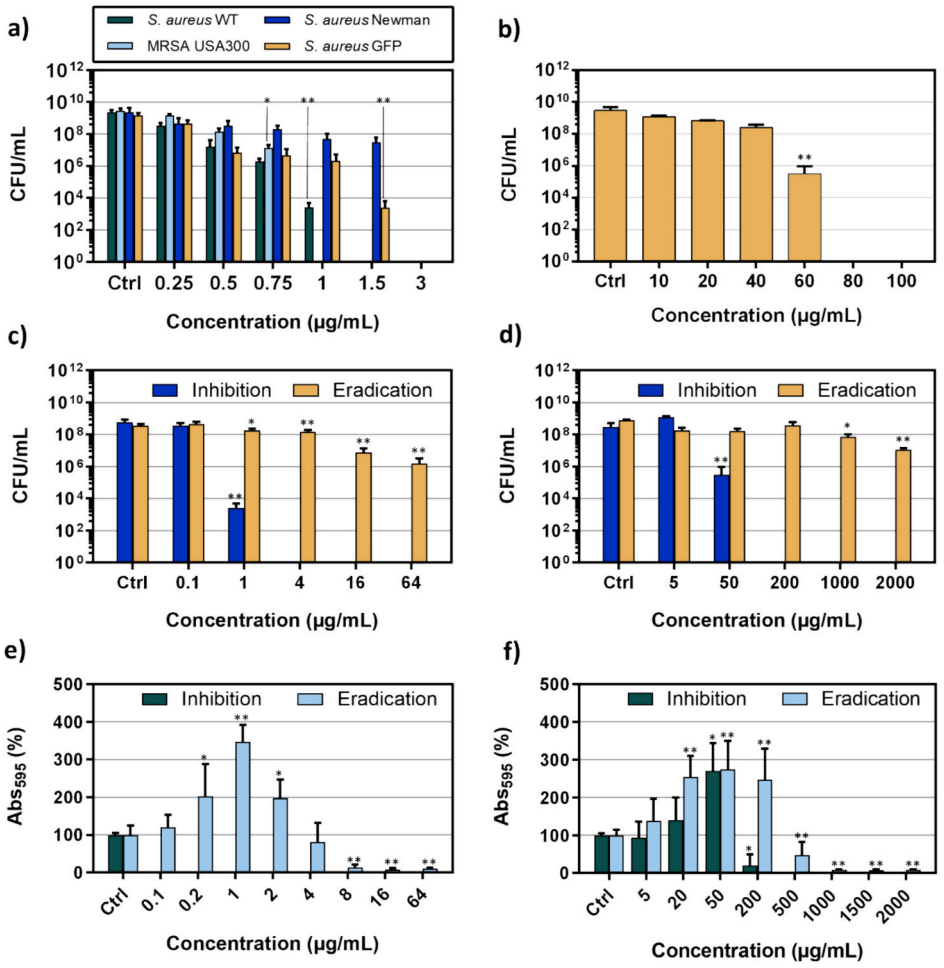

Fig. 3. Antimicrobial and antibiofilm activity of free LYS and PLGA@LYS NPs: a) Antimicrobial activity of free LYS against various strains of *S. aureus* in planktonic state; b) Antimicrobial activity of PLGA@LYS NPs against *S. aureus* GFP in planktonic state; c) Colony counting (CFU/mL) of *S. aureus* GFP obtained from biofilm inhibition and eradication studies using free LYS; d) Colony counting (CFU/mL) of *S. aureus* GFP obtained from biofilm inhibition and eradication studies using PLGA@LYS NPs; e) Biofilm biomass obtained after inhibition and eradication activity of free LYS using the crystal violet staining assay; f) Biofilm biomass obtained after inhibition and eradication activity of PLGA@LYS NPs using the crystal violet staining assay. All the experiments were performed at least three times in triplicate ($N \geq 9$). The statistics analyses compare each experimental group to the control one (*$p < 0.05$; **$p < 0.01$; ***$p < 0.001$). Ctrl displays the results obtained in both control samples evaluated (not treated and not loaded PLGA NPs) as no differences were observed.

process.

On the other hand, neither free LYS nor PLGA@LYS NPs were able to completely eliminate the bacterial population in preformed mature biofilms (Fig. 3c and d, eradication assays, respectively), though a significant reduction in the bacterial load was attained at the highest concentrations assayed. On mature biofilms, the MIC was reached for the free LYS at 16 μg/mL while for the PLGA@LYS NPs was 2000 μg/mL, which corresponds to a concentration of 57.6 μg/mL of encapsulated LYS. Conversely, the inhibition of biofilm formation was fully achieved, showing a significant reduction in the bacterial load (MIC) at concentrations of 1 μg/mL of free LYS (Fig. 3c) and at 50 μg/mL for PLGA@LYS NPs (1.44 μg/mL of encapsulated LYS; Fig. 3d), whereas biofilm formation was completely hampered at 4 μg/mL of free LYS (Fig. 3c) and at 200 μg/mL for PLGA@LYS NPs (5.76 μg/mL of encapsulated LYS; Fig. 3d). It should be noted that control samples (not treated or treated with PLGA@NPs not loaded with LYS) yielded the same results, thus PLGA did not exert any effect in bacteria nor biofilm.

The higher concentration needed to eliminate bacteria in a mature biofilm when using PLGA@LYS NPs compared to the use of the free enzyme could be attributed to the difficulty for the NPs to diffuse and permeate through the exopolysaccharide-composed biofilm during the time of our experiments (24 h). In agreement with the previous literature, the doses of antimicrobial needed to completely eradicate bacteria in mature biofilms are orders of magnitude superior to the ones needed when bacteria remain in their planktonic state [51].

In the analysis of biofilm biomass formation using the Crystal Violet assay (Fig. 3e and f), it was shown that the lowest concentration of LYS (0.1 μg/mL) was capable of inhibiting biofilm formation, while the PLGA@LYS NPs formulation required 500 μg/mL (14.4 μg/mL of encapsulated LYS) for a similar outcome. Nevertheless, considering the results of colony counting in these assays (Fig. 3c and d, inhibition assays), it should be noted that the absence of biomass due to the inhibition of biofilm formation does not always imply the complete elimination of the bacteria. For instance, even though 0.1 μg/mL of LYS was effective in preventing biofilm formation, there were still bacteria present in the cultures, even in those treated with 1 μg/mL. In contrast, for the case of PLGA@LYS NPs, the bacteria were eliminated with 200 μg/mL (5.76 μg/mL of encapsulated LYS), even though the presence of reduced biomass was still observed.

Additionally, it was observed (Fig. 3e and f) that 8 μg/mL of LYS and 500 μg/mL of PLGA@LYS NPs (14.4 μg/mL of encapsulated LYS) were needed to significantly disperse and nearly eradicate an already established mature biofilm. However, as pointed out above, neither free LYS nor PLGA@LYS NPs could completely eliminate the bacteria present in the culture, as attested in the eradication data (Fig. 3c and d). Again, control samples (not treated or treated with PLGA@NPs not loaded with

LYS) displayed the same results.

It has been reported that LYS can inhibit and eradicate *S. aureus* biofilms on artificial surfaces [52], a characteristic that has led to its recognition as a potential antimicrobial coating on clinical materials [53,54]. Moreover, the encapsulation of LYS has shown the potential to enhance the anti-biofilm capacities of the molecule when compared to its free form [34]. This is likely attributed to the protective effect against trapping and inactivation of the molecule in the biofilm microenvironment, and its sustained release from the carrier. In our case, we do not see an enhancement in the antimicrobial action when using the encapsulated LYS in the short term, which is attributed to the prolonged sustained release of the antimicrobial compound. We postulate that the use of a sustained release system would aid in any prolonged duration of the antimicrobial action and successive applications of the free LYS would not be necessary when having the nanoparticulated system here described.

Fig. 3e and f also revealed that there was an effect in which the biofilm mass increased in the presence of certain treatment concentrations, as antimicrobial exposure can promote biofilm formation [55]. This phenomenon can occur when sublethal concentrations of antimicrobial agents are used, which can stimulate bacteria to form biofilms as a protective response against the selective pressure of antimicrobials.

Biofilm formation of *S. aureus* GFP was monitored using confocal microscopy and the Calcofluor White stain (Fig. 4). Similar to previous assays, the capacity of free and encapsulated LYS to both inhibit and disperse the biofilm was evaluated. Cultures treated with PLGA NPs without LYS did not show changes compared to the control.

The concentrations utilized for these assays were selected taking into consideration the PLGA@LYS NPs drug loading and the results depicted in Fig. 3. In consonance with those results, both LYS and PLGA@LYS NPs formulations were more effective inhibiting the formation of biofilm rather than eradicating it. This situation was foreseeable since bacteria in inhibition assays started in a planktonic state and were in contact with the treatment since the beginning of the experiments hindering biofilm formation. Likewise, it was noticeable that a dose-dependent concentration in proposed treatments (free LYS or encapsulated one) led to a reduction in GFP expression and extracellular matrix labelling. Moreover, PLGA@LYS NP treatments appeared to be more effective in reducing the GFP signal, both in the inhibition and eradication assays, in comparison with those using free LYS. These results obtained in confocal microscopy support those obtained in the previous assays (Fig. 3).

3.3. Intracellular infection

To study the effects of the treatment of free LYS and PLGA@LYS NPs on a cell line infected with *S. aureus*, an intracellular infection model was developed using J774 macrophages infected with GFP-expressing *S. aureus*. As detailed above and taking into account that MIC values for *S. aureus* GFP were similar to those observed in the other strains used, *S. aureus* GFP was the strain chosen for further studies to take advantage of its visualization under confocal microscopy. Intracellular infection represents one of the most challenging scenarios where persister

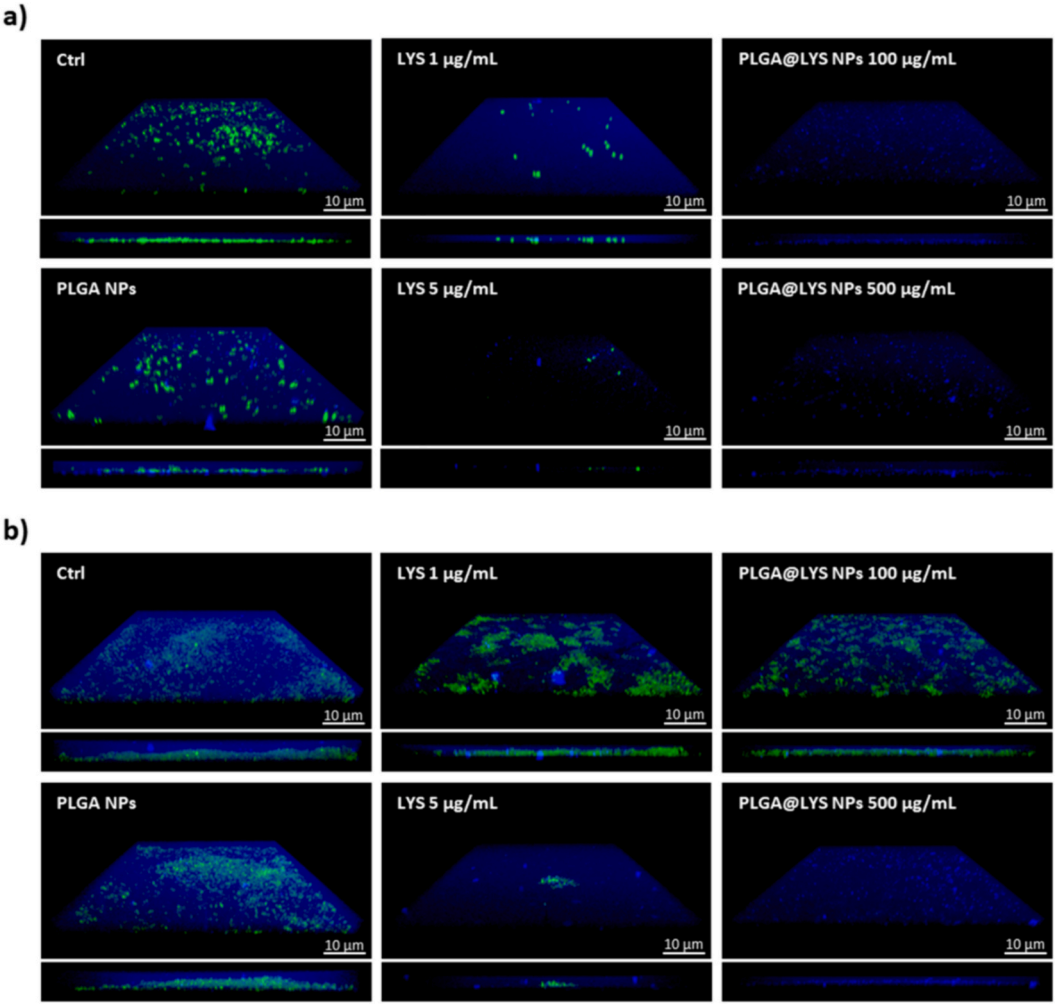

Fig. 4. Confocal laser scanning microscopy of *S. aureus* GFP biofilm cultures: a) Biofilm inhibition activity of LYS and PLGA@LYS NPs; b) Biofilm eradication activity of LYS and PLGA@LYS NPs. Control samples (biofilm not treated and treated with non-loaded PLGA NPs) were also assayed.

bacteria, named small colony variants, live intracellularly exhibiting phenotypic resistance against the action of antimicrobials and being responsible for chronic recurrent infections.

The cytotoxicity of LYS and PLGA@LYS NPs for J774 macrophages was previously assessed using the Blue Cell Viability Assay (Fig. 5). No concentration that previously demonstrated bactericidal activity caused a reduction below 80 % viability at 24 h, indicating that neither treatments could be classified as cytotoxic (according to ISO 10993-5) [56].

Fig. 6 depicts the results of employing free LYS and PLGA@LYS NPs to eradicate intracellular *S. aureus* GFP infection. Fig. 6a and b present the quantitative analysis conducted through FACS for the two strategies outlined in the methods section: pre-treatment (incubation with LYS and PLGA@LYS NPs prior to infection) and post-treatment (incubation after infection), respectively. The graphs illustrate that in both cases, around 40 to 50 % of macrophages exhibited GFP+ fluorescence, indicating their uptake of a substantial bacterial load. With the addition of LYS and PLGA@LYS NPs, the percentage of GFP+ macrophages noticeably diminished. It should be taken into account that control samples (not treated or treated with PLGA@NPs not loaded with LYS) displayed the same results, pointing to the cytocompatible character of PLGA.

In the case of the pretreatment strategy (Fig. 6a), the incubation of cells with free LYS resulted in the reduction of GFP+ macrophages to 31 %, regardless of the concentration used. However, when treated with 50 μg/mL PLGA@LYS NPs (1.44 μg/mL of LYS), GFP+ macrophages decreased to 18 %, and the addition of 100 and 500 μg/mL PLGA@LYS NPs (2.88 and 14.4 μg/mL of LYS), further lowered the count to 9 %. These results highlight how LYS encapsulation significantly enhances its antimicrobial capacity in the setting of an intracellular infection. The colocalization within the same intracellular compartment might be responsible for this high antimicrobial action observed in agreement with previous reports [57,58]. These persisters have been reported to be localized in the late endosomal/lysosomal system in macrophages [58], having the ability to resist hydrolytic enzymes, bactericidal peptides and the acidic pH [59]. Likewise, PLGA NPs are internalized by professional phagocytic cells such as macrophages and up-taken by receptor-mediated phagocytosis within the endosomal/lysosomal system [60]. Therefore, a co-localization of the nanoparticles in the same intracellular vesicle as the infective small colony variants could be responsible for the enhanced antimicrobial action observed which is of paramount relevance for their potential biomedical application. In the post-treatment strategy (Fig. 6b), it was observed how the use of 1 and 5 μg/mL of LYS decreased the amount of GFP+ infected macrophages from 48 % to 40 and 34 %, respectively. Yet, the best outcome in this context was achieved with 500 μg/mL PLGA@LYS NPs (14.4 μg/mL of LYS), resulting in a 50 % reduction of infected macrophages, and reaffirming how PLGA@LYS NPs is significantly superior to free LYS. However, it should be noted that between the two strategies, the pre-treatment approach (Fig. 6a) reduced the proportion of infected macrophages in the coculture in a more significant and prominent way.

Taking this final consideration into account, the pre-treatment strategy was chosen for a qualitative study using confocal microscopy. Fig. 6c portrays J774 macrophages infected with *S. aureus* GFP. These images utilize an orthogonal projection *via* maximum intensity projection to showcase bacteria both inside and outside cells on the same plane. *S. aureus* GFP are shown in green, while cell nuclei are stained in blue with DAPI, and the cytoskeleton is highlighted in red using phalloidin 546. The control image (infected cells with no treatment) displays the macrophages filled with green spots, suggesting a substantial load of metabolically active bacteria in the cytoplasm. The following images corroborate the outcomes from the quantitative analysis shown in Fig. 6a, highlighting how the amount of intracellular bacteria decreases more significantly and in a dose-dependent manner using PLGA@LYS NPs compared to the use of equivalent doses of the free bacteriocin.

It is reported that the bactericidal activity of LYS cannot effectively target intracellular bacteria within the host [61,62]. This is attributed to both its molecular size (~25 kDa) and by the impairment of its enzymatic activity caused by lysosomal arrest. It has been previously reported that LYS, having an optimum working pH of 7.5 shows only marginal activity at pH 6 [63]. To address this issue, Yang et al. [64] used mannose-modified exosomes as a drug delivery vehicle to deliver a combination of LYS and vancomycin, which effectively eradicated intracellular MRSA. The authors highlighted how the encapsulated formulation outperformed the free form both *in vitro* and *in vivo*. Conversely, LYS immunogenicity has been reported in human patients owing to its bacterial origin [29,65]. In this regard, previous authors have shown the increase in LYS stability when PEGylated or encapsulated into hydrogels [32–34], which may be attributed to LYS protection against host immune system hindering its recognition and internalization mediated by antigen-presenting cells. Along the same lines, Ali et al. [45] reported the development of PLGA nanoparticles incorporating the antimicrobial peptide SAAP-148, for the management of skin infection models. These particles exhibited the ability to permeate and eliminate intracellular *S. aureus* within 3D human skin models. Lastly, Dimer et al. [66] encapsulated the antibiotic clarithromycin in PLGA nanocapsules for targeting intracellular *S. aureus*. This approach significantly reduced intracellular *S. aureus* by 1000 times compared to the effect of the free drug. In RAW cells, treated bacteria shifted to non-acidic compartments. The nanocapsules demonstrated potential *in vivo* in wound models and zebrafish, indicating improved delivery to sub-epithelial tissues.

Based on the results obtained in the last part of our study, it can be concluded that the PLGA nanoencapsulation of LYS was very effective in enhancing the therapeutic efficacy of the bacteriocin to eradicate intracellular pathogens. This improvement was particularly evident with the pre-treatment strategy. Considering the background, this could be attributed to the promotion of phagocytosis, its safeguarding against lysosomal arrest, and its facilitation of accumulation within the cell

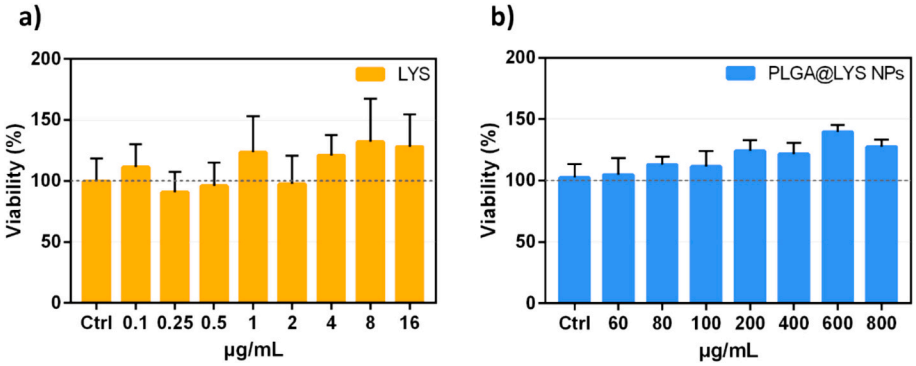

Fig. 5. J774 macrophages viability after 24 h of incubation with rising concentrations of free LYS (a) and PLGA@LYS NPs (b) following the Blue Cell Viability Assay. Experimental conditions were tested in triplicate. Ctrl displays the results obtained in both control samples evaluated (not treated and not loaded PLGA NPs) as no differences were observed.

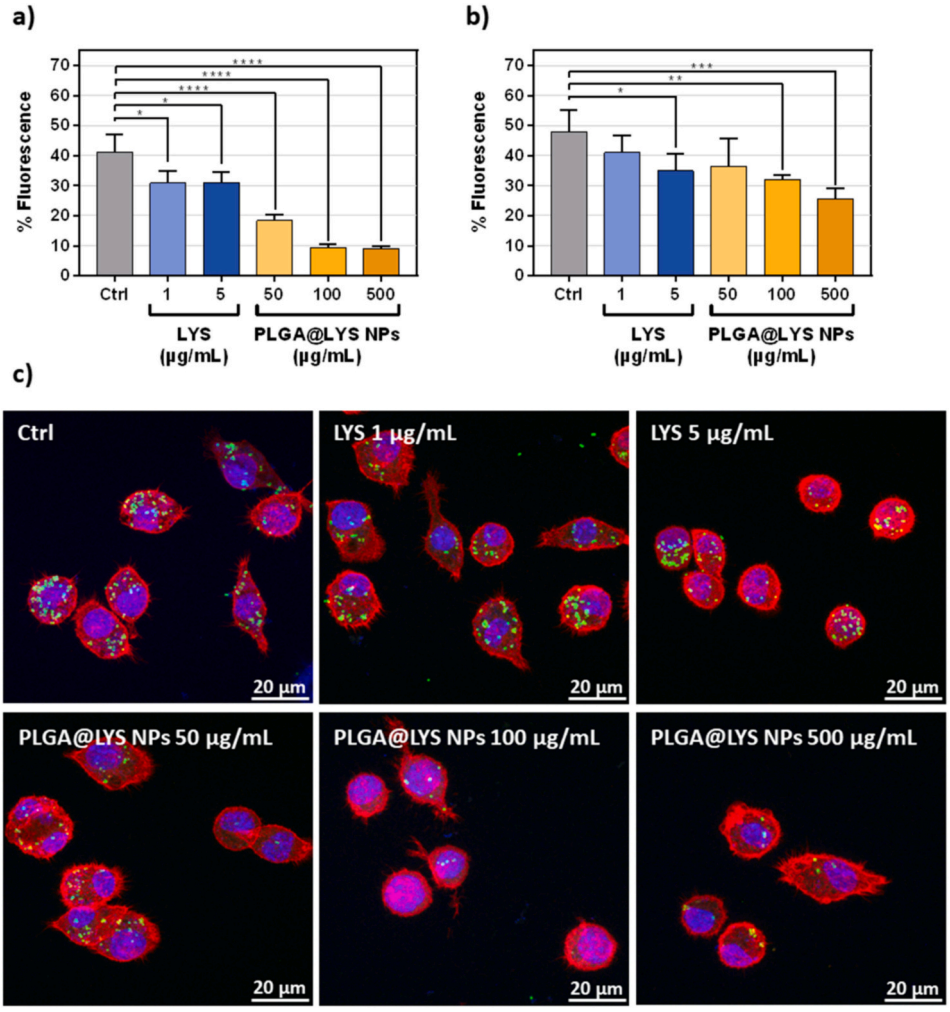

Fig. 6. Therapeutic activity of free LYS and PLGA@LYS NPs in the intracellular infection model in J774 macrophages mediated by *S. aureus* GFP: a) Flow cytometry analysis of the pre-treatment strategy assay. The graph illustrates the percentage of macrophages in the culture exhibiting GFP signal from intracellular *S. aureus* GFP; b) Flow cytometry analysis of the post-treatment strategy assay. The graph illustrates the percentage of macrophages in the culture exhibiting GFP signal from intracellular *S. aureus* GFP; c) Images of confocal laser scanning microscopy of the pre-treatment assay. *S. aureus* GFP is constitutively expressing in green, while cell nuclei were stained in blue and the cell cytoskeleton in red. Data on graphs are expressed as mean ± SD of three independent experiments. The statistics compare each experimental group *vs* the control one (*$p < 0.05$; **$p < 0.01$; ***$p < 0.001$; ****$p < 0.0001$). Ctrl displays the results obtained in both control samples evaluated (not treated and not loaded PLGA NPs) as no differences were observed.

cytoplasm.

4. Conclusion

This study achieved the successful encapsulation of LYS, an anti-*Staphylococcus aureus* bacteriocin, within stable and monodisperse PLGA nanoparticles. The obtained PLGA@LYS NPs demonstrated a rapid LYS release during an initial burst followed by a sustained release. This release kinetics is beneficial for biomedical purposes, providing a fast initial availability of LYS to eliminate bacteria while the subsequent sustained release maintains persistent concentration levels, hampering the possible further bacterial growth and re-infection. When tested against *S. aureus* cultures, the formulation retained LYS antimicrobial properties and also against biofilm cultures reducing the number of colonies and the pathogenic biomass or even completely eliminating biofilm in the inhibition assays. These results, while not identical to those obtained when bacteria were treated with free LYS, indicate that LYS retained its bactericidal activity after the encapsulation process. Moreover, it demonstrated an enhanced antimicrobial activity in an intracellular infection model of murine macrophages, both in pre-treatment and post-treatment strategies, pointing to their potential in the treatment of infections mediated by *S. aureus*. On the other hand, this study shows some limitations as the *in vitro* colocalization of PLGA@LYS NPs into the endosomal/lysosomal system has not been accurately determined and preclinical studies would elucidate the efficiency of the synthesized NPs. Therefore, further studies should be conducted to deepen into PLGA@LYS NPs bactericidal effects.

The *in vivo* limitations of the application of free LYS can be overcome by its encapsulation within PLGA-based nanoparticles to provide with a sustained release over time, a reduction in the bacterial biomass and the elimination of intracellular small colony variants responsible for episodes of infection relapse. Therefore, the developed NPs may be a promising novel strategy against biofilm and intracellular infections mediated by *S. aureus*.

CRediT authorship contribution statement

Guillermo Landa: Writing – original draft, Visualization, Validation, Software, Methodology, Formal analysis, Data curation. **Laura Aguerri:** Software, Methodology, Formal analysis, Data curation. **Silvia Irusta:** Writing – review & editing, Supervision, Resources, Investigation, Conceptualization. **Gracia Mendoza:** Writing – review & editing,

Visualization, Validation, Supervision, Methodology, Investigation. **Manuel Arruebo:** Writing – review & editing, Visualization, Supervision, Resources, Project administration, Investigation, Funding acquisition, Conceptualization.

Declaration of competing interest

The authors declare that they have no known competing financial interests or personal relationships that could have appeared to influence the work reported in this paper.

Acknowledgements

The authors acknowledge the Spanish Ministry of Science and Innovation (grant numbers PID2020-113987RB-I00 and PDC2021-121405-I00, the later founded by MCIN/AEI/10.13039/501100011033 and by the European Union "NextGenerationEU"/PRTR). We also thank the LMA-INMA (University of Zaragoza, Spain) and Technical Core Units from IACS/IIS Aragon for their instruments and expertise. G.L. acknowledges the support from the FPI program (PRE2018-085769, Spanish Ministry of Science, Innovation and Universities). G.M. gratefully acknowledges the support from the Miguel Servet Program (MS19/00092; Instituto de Salud Carlos III).

References

[1] H.F. Chambers, The changing epidemiology of *Staphylococcus aureus*? Emerg. Infect. Dis. 7 (2001) 178–182, https://doi.org/10.3201/eid0702.010204.
[2] F.R. DeLeo, M. Otto, B.N. Kreiswirth, H.F. Chambers, Community-associated meticillin-resistant *Staphylococcus aureus*, The Lancet 375 (2010) 1557–1568, https://doi.org/10.1016/S0140-6736(09)61999-1.
[3] K.S. Ikuta, L.R. Swetschinski, G. Robles Aguilar, F. Sharara, T. Mestrovic, A.P. Gray, N. Davis Weaver, E.E. Wool, C. Han, A. Gershberg Hayoon, A. Aali, S.M. Abate, M. Abbasi-Kangevari, Z. Abbasi-Kangevari, M. Naghavi, Global mortality associated with 33 bacterial pathogens in 2019: a systematic analysis for the Global Burden of Disease Study 2019, Lancet 400 (2022) 2221–2248, https://doi.org/10.1016/S0140-6736(22)02185-7.
[4] B.P. Conlon, *Staphylococcus aureus* chronic and relapsing infections: evidence of a role for persister cells, BioEssays 36 (2014) 991–996, https://doi.org/10.1002/bies.201400080.
[5] S.Y.C. Tong, J.S. Davis, E. Eichenberger, T.L. Holland, V.G. Fowler, *Staphylococcus aureus* infections: epidemiology, pathophysiology, clinical manifestations, and management, Clin. Microbiol. Rev. 28 (2015) 603–661, https://doi.org/10.1128/CMR.00134-14.
[6] H.W. Boucher, G.R. Corey, Epidemiology of methicillin-resistant *Staphylococcus aureus*, Clin. Infect. Dis. 46 (2008) S344–S349, https://doi.org/10.1086/533590.
[7] S. Roberts, S. Chambers, Diagnosis and management of *Staphylococcus aureus* infections of the skin and soft tissue, Intern. Med. J. 35 (2005) S97–S105, https://doi.org/10.1111/j.1444-0903.2005.00983.x.
[8] M. Patricia Jevons, "Celbenin" - resistant *staphylococci*, Br. Med. J. 1 (1961) 124–125.
[9] I.M. Gould, J. Reilly, D. Bunyan, A. Walker, Costs of healthcare-associated methicillin-resistant *Staphylococcus aureus* and its control, Clin. Microbiol. Infect. 16 (2010) 1721–1728, https://doi.org/10.1111/j.1469-0691.2010.03365.x.
[10] World Health Organization (WHO), Prioritization of Pathogens to Guide Discovery, Research and Development of New Antibiotics for Drug-Resistant Bacterial Infections, Including Tuberculosis, 2017.
[11] M.A. Riley, J.E. Wertz, Bacteriocins: evolution, ecology, and application, Annu. Rev. Microbiol. 56 (2002) 117–137, https://doi.org/10.1146/annurev.micro.56.012302.161024.
[12] P.D. Cotter, R.P. Ross, C. Hill, Bacteriocins — a viable alternative to antibiotics? Nat. Rev. Microbiol. 11 (2013) 95–105, https://doi.org/10.1038/nrmicro2937.
[13] H.P. Browder, W.A. Zygmunt, J.R. Young, P.A. Tavormina, Lysostaphin: enzymatic mode of action, Biochem. Biophys. Res. Commun. 19 (1965) 383–389, https://doi.org/10.1016/0006-291X(65)90473-0.
[14] C.A. Schindler, V.T. Schuhardt, Lysostaphin: a new bacteriolytic agent for the *Staphylococcus*, Proc. Natl. Acad. Sci. 51 (1964) 414–421, https://doi.org/10.1073/pnas.51.3.414.
[15] J.A. Wu, C. Kusuma, J.J. Mond, J.F. Kokai-Kun, Lysostaphin disrupts *Staphylococcus aureus* and *Staphylococcus epidermidis* biofilms on artificial surfaces, Antimicrob. Agents Chemother. 47 (2003) 3407–3414, https://doi.org/10.1128/AAC.47.11.3407-3414.2003.
[16] C.M. Kusuma, J.F. Kokai-Kun, Comparison of four methods for determining lysostaphin susceptibility of various strains of *Staphylococcus aureus*, Antimicrob. Agents Chemother. 49 (2005) 3256–3263, https://doi.org/10.1128/AAC.49.8.3256-3263.2005.
[17] R.E. Dixon, J.S. Goodman, M.G. Koenig, Lysostaphin: an enzymatic approach to staphylococcal disease. 3. Combined lysostaphin-methicillin therapy of established staphylococcal abscesses in mice, Yale J. Biol. Med. 41 (1968) 62–68.
[18] F.X. Placencia, L. Kong, L.E. Weisman, Treatment of methicillin-resistant *Staphylococcus aureus* in neonatal mice: Lysostaphin versus vancomycin, Pediatr. Res. 65 (2009) 420–424, https://doi.org/10.1203/PDR.0b013e3181994a53.
[19] M. do C. de F. Bastos, B.G. Coutinho, M.L.V. Coelho, Lysostaphin: a staphylococcal bacteriolysin with potential clinical applications, Pharmaceuticals 3 (2010) 1139–1161, https://doi.org/10.3390/ph3041139.
[20] A. Shah, J. Mond, S. Walsh, Lysostaphin-coated catheters eradicate *Staphylococccus aureus* challenge and block surface colonization, Antimicrob. Agents Chemother. 48 (2004) 2704–2707, https://doi.org/10.1128/AAC.48.7.2704-2707.2004.
[21] H. Ceotto-Vigoder, S.L.S. Marques, I.N.S. Santos, M.D.B. Alves, E.S. Barrias, A. Potter, D.S. Alviano, M.C.F. Bastos, Nisin and lysostaphin activity against preformed biofilm of *Staphylococcus aureus* involved in bovine mastitis, J. Appl. Microbiol. 121 (2016) 101–114, https://doi.org/10.1111/jam.13136.
[22] J.F. Kokai-Kun, T. Chanturiya, J.J. Mond, Lysostaphin as a treatment for systemic *Staphylococcus aureus* infection in a mouse model, J. Antimicrob. Chemother. 60 (2007) 1051–1059, https://doi.org/10.1093/jac/dkm347.
[23] A.P. Desbois, C.G. Gemmell, P.J. Coote, In vivo efficacy of the antimicrobial peptide ranalexin in combination with the endopeptidase lysostaphin against wound and systemic meticillin-resistant *Staphylococcus aureus* (MRSA) infections, Int. J. Antimicrob. Agents 35 (2010) 559–565, https://doi.org/10.1016/j.ijantimicag.2010.01.016.
[24] C.T. Johnson, M.C.P. Sok, K.E. Martin, P.P. Kalelkar, J.D. Caplin, E.A. Botchwey, A. J. García, Lysostaphin and BMP-2 co-delivery reduces *S. Aureus* infection and regenerates critical-sized segmental bone defects, Sci. Adv. 5 (2019), https://doi.org/10.1126/sciadv.aaw1228.
[25] M.W. Climo, R.L. Patron, B.P. Goldstein, G.L. Archer, Lysostaphin treatment of experimental methicillin-resistant *Staphylococcus aureus* aortic valve endocarditis, Antimicrob. Agents Chemother. 42 (1998) 1355–1360, https://doi.org/10.1128/AAC.42.6.1355.
[26] J.J. Dajcs, B.A. Thibodeaux, D.O. Girgis, M.D. Shaffer, S.M. Delvisco, R. J. O'Callaghan, Immunity to lysostaphin and its therapeutic value for ocular MRSA infections in the rabbit, Invest. Ophthalmol. Vis. Sci. 43 (2002) 3712–3716.
[27] B. Xue, C. Zhang, Y. Wang, J. Wang, J. Zhang, M. Lu, G. Li, Z. Cao, Q. Huang, A novel controlled-release system for antibacterial enzyme lysostaphin delivery using hydroxyapatite/chitosan composite bone cement, PloS One 9 (2014) e113797, https://doi.org/10.1371/journal.pone.0113797.
[28] K.E. Quickel, R. Selden, J.R. Caldwell, N.F. Nora, W. Schaffner, Efficacy and safety of topical lysostaphin treatment of persistent nasal carriage of *Staphylococcus aureus*, Appl. Microbiol. 22 (1971) 446–450, https://doi.org/10.1128/am.22.3.446-450.1971.
[29] J. Jayakumar, V.A. Kumar, L. Biswas, R. Biswas, Therapeutic applications of lysostaphin against *Staphylococcus aureus*, J. Appl. Microbiol. 131 (2021) 1072–1082, https://doi.org/10.1111/jam.14985.
[30] M. Drayton, J.N. Kizhakkedath, S.K. Strau, Towards robust delivery of antimicrobial peptides to combat bacterial resistance, Molecules 25 (2020) 1–24, https://doi.org/10.3390/molecules25133048.
[31] M.J. Daley, E.R. Oldham, Lysostaphin: immunogenicity of locally administered recombinant protein used in mastitis therapy, Vet. Immunol. Immunopathol. 31 (1992) 301–312, https://doi.org/10.1016/0165-2427(92)90017-K.
[32] S. Walsh, A. Shah, J. Mond, Improved pharmacokinetics and reduced antibody reactivity of Lysostaphin conjugated to polyethylene glycol, Antimicrob. Agents Chemother. 47 (2003) 554–558, https://doi.org/10.1128/AAC.47.2.554-558.2003.
[33] G. Resch, P. Moreillon, V.A. Fischetti, PEGylating a bacteriophage endolysin inhibits its bactericidal activity, AMB Express 1 (2011) 29, https://doi.org/10.1186/2191-0855-1-29.
[34] C.T. Johnson, J.A. Wroe, R. Agarwal, K.E. Martin, R.E. Guldberg, R.M. Donlan, L. F. Westblade, A.J. García, Hydrogel delivery of lysostaphin eliminates orthopedic implant infection by *Staphylococcus aureus* and supports fracture healing, Proc. Natl. Acad. Sci. 115 (2018), https://doi.org/10.1073/pnas.1801013115.
[35] C.-Y. Huang, J.-T. Hsu, P.-H. Chung, W.T.-K. Cheng, Y.-N. Jiang, Y.-T. Ju, Site-specific N-glycosylation of caprine lysostaphin restricts its bacteriolytic activity toward *Staphylococcus aureus*, Anim. Biotechnol. 24 (2013) 129–147, https://doi.org/10.1080/10495398.2012.760469.
[36] X. Lin, J. He, W. Li, Y. Qi, H. Hu, D. Zhang, F. Xu, X. Chen, M. Zhou, Lung-targeting Lysostaphin microspheres for methicillin-resistant *Staphylococcus aureus* pneumonia treatment and prevention, ACS Nano 15 (2021) 16625–16641, https://doi.org/10.1021/acsnano.1c06460.
[37] F. Cui, G. Li, J. Huang, J. Zhang, M. Lu, W. Lu, J. Huan, Q. Huang, Development of chitosan-collagen hydrogel incorporated with lysostaphin (CCHL) burn dressing with anti-methicillin-resistant *Staphylococcus aureus* and promotion wound healing properties, Drug Deliv. 18 (2011) 173–180, https://doi.org/10.3109/10717544.2010.509363.
[38] A.V. Grishin, N.V. Shestak, N.V. Lavrova, A.M. Lyashchuk, L.I. Popova, N. V. Strukova, M.S. Generalova, A.V. Ryazanova, N.B. Polyakov, Z.M. Galushkina, L. A. Soboleva, I.S. Boksha, A.S. Karyagina, V.G. Lunin, Fusion of Lysostaphin to an albumin binding domain prolongs its half-life and bactericidal activity in the systemic circulation, Molecules 24 (2019) 2892, https://doi.org/10.3390/molecules24162892.
[39] S.C. Becker, D.R. Roach, V.S. Chauhan, Y. Shen, J. Foster-Frey, A.M. Powell, G. Bauchan, R.A. Lease, H. Mohammadi, W.J. Harty, C. Simmons, M. Schmelcher, M. Camp, S. Dong, J.R. Baker, T.R. Sheen, K.S. Doran, D.G. Pritchard, R. A. Almeida, D.C. Nelson, I. Marriott, J.C. Lee, D.M. Donovan, Triple-acting lytic

enzyme treatment of drug-resistant and intracellular *Staphylococcus aureus*, Sci. Rep. 6 (2016) 25063, https://doi.org/10.1038/srep25063.
[40] Z. Wang, L. Kong, Y. Liu, Q. Fu, Z. Cui, J. Wang, J. Ma, H. Wang, Y. Yan, J. Sun, A phage Lysin fused to a cell-penetrating peptide kills intracellular methicillin-resistant *Staphylococcus aureus* in keratinocytes and has potential as a treatment for skin infections in mice, Appl. Environ. Microbiol. 84 (2018), https://doi.org/10.1128/AEM.00380-18.
[41] C. Röhrig, M. Huemer, D. Lorgé, S. Luterbacher, P. Phothaworn, C. Schefer, A. M. Sobieraj, L.V. Zinsli, S. Mairpady Shambat, N. Leimer, A.P. Keller, F. Eichenseher, Y. Shen, S. Korbsrisate, A.S. Zinkernagel, M.J. Loessner, M. Schmelcher, Targeting hidden pathogens: cell-penetrating enzybiotics eradicate intracellular drug-resistant *Staphylococcus aureus*, MBio 11 (2020), https://doi.org/10.1128/mBio.00209-20.
[42] F. Hajiahmadi, M.Y. Alikhani, H. Shariatifar, M.R. Arabestani, D. Ahmadvand, The bactericidal effect of lysostaphin coupled with liposomal vancomycin as a dual combating system applied directly on methicillin-resistant *Staphylococcus aureus* infected skin wounds in mice, Int. J. Nanomedicine 14 (2019) 5943–5955, https://doi.org/10.2147/IJN.S214521.
[43] N.R. Mohamad, N.H.C. Marzuki, N.A. Buang, F. Huyop, R.A. Wahab, An overview of technologies for immobilization of enzymes and surface analysis techniques for immobilized enzymes, Biotechnol. Biotechnol. Equip. 29 (2015) 205–220, https://doi.org/10.1080/13102818.2015.1008192.
[44] D. Blanco, M.J. Alonso, Protein encapsulation and release from poly(lactide-co-glycolide) microspheres: effect of the protein and polymer properties and of the co-encapsulation of surfactants, Eur. J. Pharm. Biopharm. 45 (1998) 285–294, https://doi.org/10.1016/S0939-6411(98)00011-3.
[45] M. Ali, M.E. van Gent, A.M. de Waal, B.R. van Doodewaerd, E. Bos, R.I. Koning, R. A. Cordfunke, J.W. Drijfhout, P.H. Nibbering, Physical and functional characterization of PLGA nanoparticles containing the antimicrobial peptide SAAP-148, Int. J. Mol. Sci. 24 (2023) 2867, https://doi.org/10.3390/ijms24032867.
[46] X. Lin, J. He, W. Li, Y. Qi, H. Hu, D. Zhang, F. Xu, X. Chen, M. Zhou, Lung-targeting Lysostaphin microspheres for methicillin-resistant *Staphylococcus aureus* pneumonia treatment and prevention, ACS Nano 15 (2021) 16625–16641, https://doi.org/10.1021/acsnano.1c06460.
[47] D. Essa, P.P.D. Kondiah, Y.E. Choonara, V. Pillay, The design of poly(lactide-co-glycolide) nanocarriers for medical applications, Front. Bioeng. Biotechnol. 8 (2020), https://doi.org/10.3389/fbioe.2020.00048.
[48] S. Garcia-Salinas, E. Gámez, G. Landa, M. Arruebo, S. Irusta, G. Mendoza, Antimicrobial wound dressings against fluorescent and methicillin-sensitive intracellular pathogenic bacteria, ACS Appl. Mater. Interfaces 12 (2020) 51302–51313, https://doi.org/10.1021/acsami.0c17043.
[49] G.-H. Zhang, R.-X. Hou, D.-X. Zhan, Y. Cong, Y.-J. Cheng, J. Fu, Fabrication of hollow porous PLGA microspheres for controlled protein release and promotion of cell compatibility, Chin. Chem. Lett. 24 (2013) 710–714, https://doi.org/10.1016/j.cclet.2013.05.011.
[50] M.M. Huber, T.W. Huber, Susceptibility of methicillin-resistant *Staphylococcus aureus* to lysostaphin, J. Clin. Microbiol. 27 (1989) 1122–1124, https://doi.org/10.1128/jcm.27.5.1122-1124.1989.
[51] H. Hirt, S.-U. Gorr, Antimicrobial peptide GL13K is effective in reducing biofilms of *Pseudomonas aeruginosa*, Antimicrob. Agents Chemother. 57 (2013) 4903–4910, https://doi.org/10.1128/AAC.00311-13.
[52] J.A. Wu, C. Kusuma, J.J. Mond, J.F. Kokai-Kun, Lysostaphin disrupts *Staphylococcus aureus* and *Staphylococcus epidermidis* biofilms on artificial surfaces, Antimicrob. Agents Chemother. 47 (2003) 3407–3414, https://doi.org/10.1128/AAC.47.11.3407-3414.2003.
[53] A. Shah, J. Mond, S. Walsh, Lysostaphin-coated catheters eradicate *Staphylococccus aureus* challenge and block surface colonization, Antimicrob. Agents Chemother. 48 (2004) 2704–2707, https://doi.org/10.1128/AAC.48.7.2704-2707.2004.
[54] B.A. Taş, E. Berksun, C.E. Taş, S. Ünal, H. Ünal, Lysostaphin-functionalized waterborne polyurethane/polydopamine coatings effective against *S. Aureus* biofilms, ACS Appl. Polym. Mater. 4 (2022) 4298–4305, https://doi.org/10.1021/acsapm.2c00254.
[55] J.B. Kaplan, Antibiotic-induced biofilm formation, Int. J. Artif. Organs 34 (2011) 737–751, https://doi.org/10.5301/ijao.5000027.
[56] ISO 10993-5:2009, Biological Evaluation of Medical Devices — Part 5: Tests for in Vitro Cytotoxicity 3, 2009.
[57] V. Andreu, A. Larrea, P. Rodriguez-Fernandez, S. Alfaro, B. Gracia, A. Lucía, L. Usón, A.-C. Gomez, G. Mendoza, A. Lacoma, J. Dominguez, C. Prat, V. Sebastian, J.A. Ainsa, M. Arruebo, Matryoshka-type gastro-resistant microparticles for the oral treatment of *mycobacterium tuberculosis*, Nanomedicine 14 (2019) 707–726, https://doi.org/10.2217/nnm-2018-0258.
[58] A. Lacoma, L. Usón, G. Mendoza, V. Sebastián, E. Garcia-Garcia, B. Muriel-Moreno, J. Domínguez, M. Arruebo, C. Prat, Novel intracellular antibiotic delivery system against *Staphylococcus aureus*: cloxacillin-loaded poly(*d*, *l*-lactide-co-glycolide) acid nanoparticles, Nanomedicine 15 (2020) 1189–1203, https://doi.org/10.2217/nnm-2019-0371.
[59] A. Schröder, R. Kland, A. Peschel, C. von Eiff, M. Aepfelbacher, Live cell imaging of phagosome maturation in *Staphylococcus aureus* infected human endothelial cells: small colony variants are able to survive in lysosomes, Med. Microbiol. Immunol. 195 (2006) 185–194, https://doi.org/10.1007/s00430-006-0015-0.
[60] S. Behzadi, V. Serpooshan, W. Tao, M.A. Hamaly, M.Y. Alkawareek, E.C. Dreaden, D. Brown, A.M. Alkilany, O.C. Farokhzad, M. Mahmoudi, Cellular uptake of nanoparticles: journey inside the cell, Chem. Soc. Rev. 46 (2017) 4218–4244, https://doi.org/10.1039/C6CS00636A.
[61] H.W. Barkema, Y.H. Schukken, R.N. Zadoks, Invited review: the role of cow, pathogen, and treatment regimen in the therapeutic success of bovine *Staphylococcus aureus* mastitis, J. Dairy Sci. 89 (2006) 1877–1895, https://doi.org/10.3168/jds.S0022-0302(06)72256-1.
[62] E.R. Oldham, M.J. Daley, Lysostaphin: use of a recombinant bactericidal enzyme as a mastitis therapeutic, J. Dairy Sci. 74 (1991) 4175–4182, https://doi.org/10.3168/jds.S0022-0302(91)78612-8.
[63] I. Sabala, I.-M. Jonsson, A. Tarkowski, M. Bochtler, Anti-staphylococcal activities of lysostaphin and LytM catalytic domain, BMC Microbiol. 12 (2012) 97, https://doi.org/10.1186/1471-2180-12-97.
[64] X. Yang, B. Xie, H. Peng, G. Shi, B. Sreenivas, J. Guo, C. Wang, Y. He, Eradicating intracellular MRSA via targeted delivery of lysostaphin and vancomycin with mannose-modified exosomes, J. Control. Release 329 (2021) 454–467, https://doi.org/10.1016/j.jconrel.2020.11.045.
[65] J.F. Kokai-Kun, Lysostaphin: A silver bullet for staph, in: Antimicrobial Drug Discovery: Emerging Strategies, CABI, Wallingford, 2012, pp. 147–165, https://doi.org/10.1079/9781845939434.0147.
[66] F. Anversa Dimer, C. de Souza Carvalho-Wodarz, A. Goes, K. Cirnski, J. Herrmann, V. Schmitt, L. Pätzold, N. Abed, C. De Rossi, M. Bischoff, P. Couvreur, R. Müller, C.-M. Lehr, PLGA nanocapsules improve the delivery of clarithromycin to kill intracellular *Staphylococcus aureus* and *mycobacterium abscessus*, Nanomedicine 24 (2020) 102125, https://doi.org/10.1016/j.nano.2019.102125.